Optik 124 (2013) 4110–4116

Contents lists available at ScienceDirect

Optik

journal homepage: www.elsevier.de/ijleo

Solder joint inspection based on neural network combined with genetic algorithm

Wu Hao, Zhang Xianmin*, Kuang Yongcong, Ouyang Gaofei, Xie Hongwei

School of Mechanical and Automotive Engineering, South China University of Technology, Guangzhou, China

ARTICLE INFO

Article history:
Received 14 July 2012
Accepted 10 December 2012

Keywords:
Automatic optical inspection
Feature selection
Genetic algorithm
Neural network
Solder joint
Printed circuit board (PCB)

ABSTRACT

To improve the performance of automatic optical inspection (AOI), a neural network combined with genetic algorithm for the diagnosis of solder joint defects on printed circuit boards (PCBs) assembled in surface mounting technology (SMT) is presented. Six types of solder joint have been classified in respect to the reality in the manufacture. The images of solder joint under test are acquired and 14 features are extracted as input features for the classification. The neural network is easily become over-fitting because these input features are not independent of each other, so the genetic algorithm is introduced to select and remove redundant input features. The experimental results have proved that the neural network combined with genetic algorithm reduced the number of input feature and had a satisfying recognition rate.

1. Introduction

Surface mount technology (SMT) has been widely used in the electronics industry. But because the size of the components is becoming smaller and packaging density of the printed circuit boards (PCBs) deceased greatly [1], the tradition manual visual inspection cannot get a satisfying result as usual. Hence automated optical inspection (AOI) has been introduced to the surface mount technology in production.

Besl and Jain [2] conducted one of the earliest studies on solder joint inspection using diffusive light in order to avoid saturated image caused by a specular reflection of the solder surface. The study and extract features of solder from the low contrast gray images has been made [3,4], however, the results were discouraging due to their sensitivity to illumination conditions.

Kim et al. [5] used three layers of ring-shaped LED at different illumination angles and a CCD camera to take gray-level images. The classification was designed as two stages. The characteristic 2D features with simpler computation were extracted and input to a back propagation neural network for classification at the first stage. If the output value was not in the confidence, a computationally expensive algorithm based on the 3D features with a Bayes classifier would be used. The experimental results showed that the proposed methods had a good performance in both speed and recognition rate.

H.H. Loh, [6] developed a slant map surface shape estimation technique for the solder joint. A novel structured-lighting inspection technology was presented. A solder joint can be determined to be a good (concave), bad (convex), bridged solder joint, or solder joint with surplus solder, or lacking solder.

Chiu and Peng [7] presented a new approach that required only one layer of tired light, and its classification method made use of only two features so that insufficient, acceptable and excessive solders can be divided into three classes by two straight lines on the two-dimensional feature plane. These features were derived step by step from well-established physical laws, though only in qualitative sense.

G. Acciani [8] presented a neural network-based automatic optical inspection system for the diagnosis of solder joint defects. Five types of solder joints have been classified in respect to the amount of solder paste in order to perform the diagnosis with high recognition, and 10 geometric features and 8 wavelet features were extracted. The results have been proved that the MLP network fed with the GW-features had the best recognition rate.

Although the inspection methods mentioned above with new features have a high speed at the experiment, but the types of solder joints can only focus on the volume of soldering such as good solder, insufficient solder, excess solder, and no solder. Defects such as cold solder, tombstone, component shift, and wrong component are quite common in industrial field. This paper focuses on five most common defects of solder joint in industry. 14 features are extracted and treated as input variables of the back propagation

---

* Corresponding author.
E-mail addresses: wuhaomoses@gmail.com (W. Hao), zhangxm08@gmail.com (Z. Xianmin), yckuang@scut.edu.cn (K. Yongcong), scut_gaofei@yahoo.com.cn (O. Gaofei), xhw_cn@foxmail.com (X. Hongwei).

0030-4026/$ – see front matter © 2013 Elsevier GmbH. All rights reserved.
http://dx.doi.org/10.1016/j.ijleo.2012.12.030

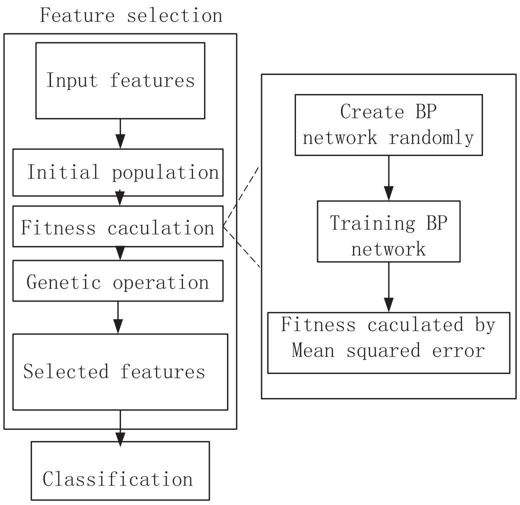

Fig. 1. Inspection procedure.

(BP) network in the beginning. Since these input variables are not independent to each other, the BP network easily becomes overfitting, both the correct accuracy and modeling time cannot get a satisfying result, so the genetic algorithm is introduced to remove redundant input features.

This paper is organized as following. In Section 2, the overall proposed method is described. In Section 3, the illumination system and the image of solder joint with different defects are presented. In Section 4, feature extraction, feature selection and the classification are described. Experimental results are obtained with the proposed method using a set of solder images in Section 5. Finally, the conclusions are made at the end of this paper.

2. Methodology

In this section, the presented approach of this paper is shown in Fig. 1.

The input features including 14 features are extracted from the solder joint area, the main procedure is constituted by the feature selection, parameter optimization and classification. The feature selection is implemented by the genetic algorithm, which is shown in the left part in Fig. 1, and the fitness is calculated by the mean squared error of the BP network, which is shown in right part in Fig. 1. Finally, the classification result is got based on the selected features.

3. Image acquirement and solder class definition

The images are obtained by a CCD color digital camera and a 3-color (red, green, and blue) hemispherical LED array illumination, which is shown in Fig. 2 [9].

The surface of the solder joint holds the same property of flat mirror, which abides to the law of reflection. The red, green, and blue lights irradiate to the flat, the slow slant, and the rapid slant of the solder joint surfaces, which are reflected to the camera respectively [10]. With such a 3-color illumination and color camera system, the 3D shape information of the solder joints can be depicted by a 2D color image. The image acquisition process is shown in Fig. 3.

Fig. 4 shows the image of the solder joint and the solder model used in this paper, the types of solder joint to be inspected includes good solder (Gs), cold solder (Cs), solder insufficient (Si), component shifted (Ct), wrong component (Wc) and tombstone (Tb). Typical images of various solder joints are shown in Table 1.

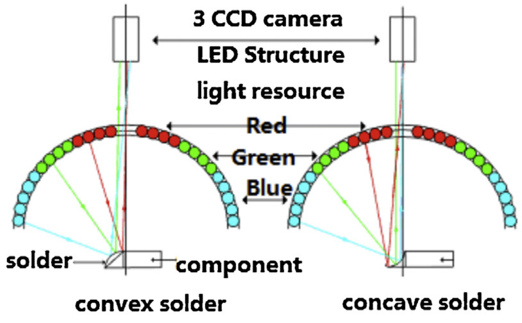

Fig. 2. 3-Color LED array illumination system.

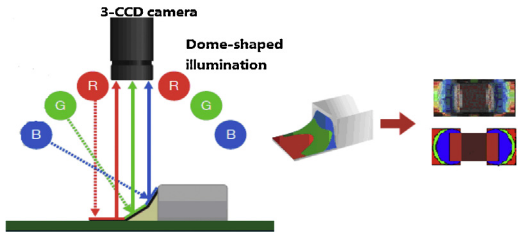

Fig. 3. The image acquisition system.

4. Feature extraction and selection

4.1. Feature extraction

From the image acquisition process before, the difference in various solder joint defects is concentrated on two areas that the component body and the problem solder pad, and there are 14 features together in these two areas. Seven features are extracted every single area, which is defined as follows:

$$X_1 = \frac{1}{M \times N} \sum_{x=1}^{M} \sum_{y=1}^{N} I_r(x, y) \tag{1}$$

$$X_2 = \frac{1}{M \times N} \sum_{x=1}^{M} \sum_{y=1}^{N} I_g(x, y) \tag{2}$$

$$X_3 = \frac{1}{M \times N} \sum_{x=1}^{M} \sum_{y=1}^{N} I_b(x, y) \tag{3}$$

$I_r(x, y)$ is the intensity of the image in the red color frame. $I_g(x, y)$ is the intensity of the image in the green color frame. $I_b(x, y)$ is the intensity of the image in the blue color frame [11], $M \times N$ is the number of pixels in the solder region. X_1, X_2, and X_3

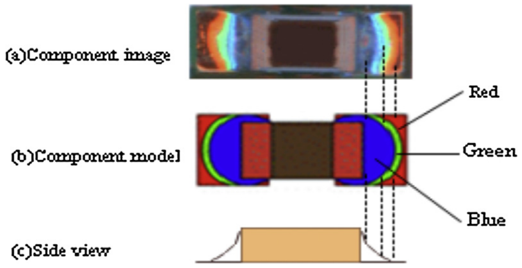

Fig. 4. The solder joint image and model.